Attempt to correlate simulations and measurements of turbine performance under pulsating flows for automotive turbochargers

Authors:

Calogero Avola[1+], Colin Copeland[1], Alessandro Romagnoli[2], Richard Burke[1] and Pavlos Dimitriou[1]

[1] Department of Mechanical Engineering, University of Bath, UK

[2] School of Mechanical and Aerospace Engineering, Nanyang Technological University, Singapore

Corresponding Author:

[+] Department of Mechanical Engineering, University of Bath, Claverton Down, BA2 7AY, UK

Email: c.avola@bath.ac.uk

Abstract

The paper attempts to correlate simulations and measurements of turbine performance under pulsating flows for automotive turbochargers. Under real automotive powertrain conditions, turbochargers are subjected to pulsating flows, due to the engine valves motions. Experiments on a purposively built 2.2L Diesel engine gas-stand have allowed quantification of unsteady pulsating turbine performance. Temperature, pressure and mass flow measurements are fundamental for the characterisation of turbine performance. Adequate sampling frequency of instruments and acquisition rates are highly important for the quantification of unsteady turbomachine performance. However, in the absence of fast responsive sensors for monitoring mass flow and temperature, appropriate considerations would have be made to perform estimates of turbine performance under pulsating flows.

A 1D model of the engine gas-stand has been developed and validated against experimental data. In the research paper, a hybrid unsteady/quasi-steady turbine model has been adopted to identify unsteadiness at turbine inlet and outlet. In order to evaluate isentropic turbine efficiency and reduce influence of external heat transfer to measurements [1], turbine inlet temperature has been measured experimentally in the vicinity of the turbine rotor in the inlet section upstream the turbine tongue. The hybrid unsteady/quasi-steady turbine model considers the presence of unsteady flows in the turbine inlet and outlet, leaving the rest of the turbine to react quasi-steadily. Furthermore, virtual sensors and thermocouples have been implemented into the 1D model to correlate experimental time-averaged temperature measurements.

Keywords: Unsteady flow; Turbine efficiency; Turbocharger; Turbine model; Turbine; Temperature

Nomenclature

1D	One-dimensional
ave	Average
CAD	Crank Angle Degree
CBP	Compressor Back-Pressure
EGR	Exhaust Gas Recirculation
I/C	Inter-cooler
inst	Instantaneous
MAF	Mass Air Flow
P	Pressure
PR	Pressure ratio

T	Temperature
TC	Thermocouple
TIT	Turbine Inlet Temperature
TOT	Turbine Outlet Temperature
VGT	Variable Geometry Turbine
VTC	Virtual Thermocouple
VTS	Virtual Temperature Sensor

1. Introduction

The use of turbochargers in conjunction with reciprocating internal combustion engines are able to provide benefits to the system for constant and transient conditions [2] and to the release of harmful pollutants into the environment through the engine tailpipe [3]. The perfect matching of turbochargers to the engine for satisfying the breathing characteristics is possible though an accurate preliminary analysis of turbocharger performance [4]. In a turbocharger, compressor and turbine performance are evaluated in test gas-stands working under steady flows [5]. In the case of a turbine, swallowing capacity and efficiency maps are generated at constant turbine speed lines linking pressure, temperature and mass flow measurements. In this scenario, steady performance maps are considered for an engine system analysis and an initial performance evaluation of automotive powertrains [6, 7]. The presence of pulsating flows at the turbine inlet can vary the operating conditions of the turbine from quasi-steady to fully unsteady, reducing the relevance of steady performance maps [8]. In engine gas-stands, pulsating flows at the turbine inlet of automotive turbochargers can be applied, allowing the analysis of performance and the change in quasi-steady conditions [9].

In the presence of unsteady flows in turbocharger turbine, performance measurements through the use of external instrumentations are significantly dependant on the positioning [10, 11]. Furthermore, deviation from steady efficiency is significant due to the presence of oscillating flow parameters in relation to operating pulsation amplitude and frequency [12, 13]. Due to the impossibility of measuring turbocharger torque, turbine efficiency is correlated to inlet and outlet temperature measurements [4]. Owing to the effect of waving flows [14], standard thermocouples have difficulties in monitoring instantaneous flow temperature, allowing the availability of time-averaged data solely. In this case, taking into account the compressor power in the turbocharger can remove the uncertainty of turbine outlet temperature from the turbine efficiency equation [15]. Therefore, the development of monitoring equipment for measuring instantaneous flow temperature [16] and the adoption of instantaneous torque meters on turbocharger shaft [17] can be considered valuable attempts for capturing unsteady turbine efficiency experimentally. In conjunction with temperature measurements of unsteady flows, increased difficulty is added for instantaneous mass flow measurement at hot turbine conditions [18]. In fact, investigations have been performed in turbocharger gas-stands incorporating pulsating devices at the turbine inlet [19]. In these cases, instantaneous mass flow measurements have shown differences on turbine hysteresis loops and average performance between straight ducts and bends at the turbine inlet, emulating the effect of an engine exhaust manifold [20].

The oscillation of pressure at turbine inlet affects the turbine behaviour and attempts in modelling the expansion process have been performed, monitoring instantaneous turbine torque at the shaft [11]. Wave actions and filling and emptying models to account for pulsating turbines have been developed, obtaining agreement between predictions and experimental data available. Models presented in Serrano et al. [21], Piscaglia et al. [22] and Chiong et al. [23] can be implemented in 1D codes and are able to account for flow pulsations generated by internal combustion engines.

However, in order to obtain useful agreements, the coupling between turbine rotor, stator and diffuser has to be accurately tuned against turbine experimental [24] and geometrical data [25]. On the other hand, the exclusion of steady turbine map from turbine model could be a lengthy process to obtain significant benefits in unsteady performance definitions of turbocharger turbine [26]. In addition, degree of complexity is increased in fully unsteady turbine models and performance could be poorly predicted under unequal flow admissions for twin and double entry turbocharger turbines [27]. Whereas, extended mapping of twin and double entry turbocharger turbines is able to capture unsteady performance [28], as a quasi-steady assumption of the turbine rotor could be able to model turbochargers turbine behaviour [29].

In this paper, a hybrid unsteady/quasi-steady model of the turbine is presented and developed in order to predict turbocharger turbine performance under unsteady flows in 1D models. On-engine applications are investigated through experiments and validations of 2.2L Diesel engine gas-stand [10]. In order to evaluate isentropic turbine efficiency and reduce heat transfer effects [1], inlet temperature at the turbine rotor has been experimentally measured and compared to measurements at the exhaust manifold. This has improved the correlation of unsteady turbine performance between engine experiments and 1D model simulations. In the proposed turbine model, unlike other turbine models [24], tuning is not necessary due to geometrical representation of turbine tongue and diffuser through tapered ducts, accounting for the turbine mass storage and pressure wave dynamics. Furthermore, virtual sensors and thermocouples have been implemented into the 1D model representing the 2.2L Diesel engine gas-stand to correlate experimental time-averaged temperature measurements. Unsteady turbocharger turbine performance are measured experimentally in the engine gas-stand at 15 operating conditions and three turbocharger speeds. In relation to the on-engine experimental data

recorded, the hybrid unsteady-quasi steady turbine model has sensibly improved the prediction of turbine outlet temperature over the quasi-steady approach.

2 Experimental evaluation

2.1 Engine gas-stand layout

In order to investigate turbine performance under pulsating conditions, an engine gas-stand facility has been developed, as visible in [10]. In fact, exhaust gasses of a four-cylinder 2.2-litre Diesel engine provide power to the 41 mm variable geometry turbine (VGT), leading to rotation of the turbocharger. As shown in figure 1, an external back-pressure (CBP) valve is generating load on the compressor, operating under steady flow. Furthermore, in order to obtain a precise control of the turbine, engine intake conditions and fuel flow rate allow variation of the exhaust conditions. In fact, a boost rig unit connected to the engine intake is able to target temperature, pressure and mass flow through a series of valves, defined as hot, dump and main valves, respectively [10].

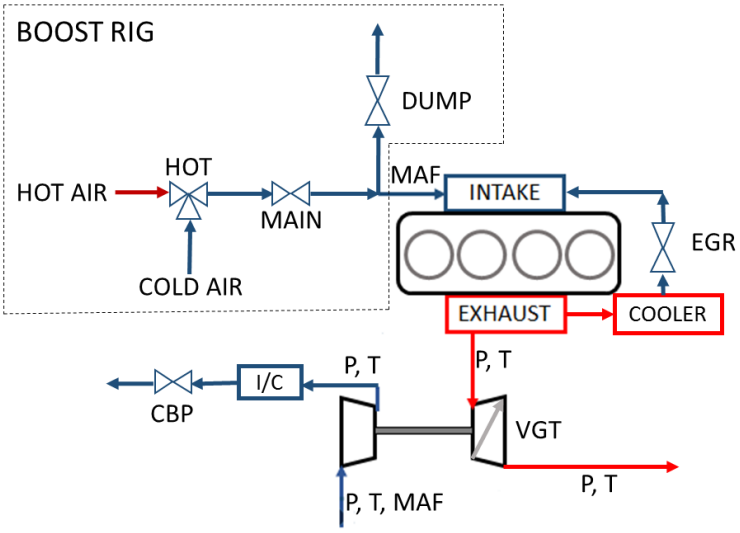

Figure 1. Engine gas-stand for investigating automotive turbochargers

Table 1. List of sensors adopted in the engine gas-stand, including range, accuracy, response and sampling frequency of sensors and acquisition system

SENSOR	RANGE	ACCURACY	RESPONSE	ACQUISITION
PRT	-50 to +200 degC	±0.3 + 0.005*T	0.04 Hz in air 1.66 Hz in water	1 Hz
K type TC	-200 to 1260 degC	0.0075*T	1.66 Hz in water for 3mm 3.33 Hz in water for 1.5mm	1 Hz
MAF	0 to 1200 kg/h	1%	82 Hz	1 Hz
Fuel flow	0 to 200 kg/h	±0.05%	1 Hz	1 Hz
Slow-sample Pressure	0 barA to 6 barA	0.25%	100 Hz	1 Hz
Fast-sample Pressure	0 barA to 5 barA	0.3%	500 kHz	120 kHz (engine at 2000 rpm)
Turbo speed	0 to 400,000 rpm	0.1%	100 kHz	120 kHz (engine at 2000 rpm)

Turbine performance can be monitored as pressure, temperature and mass flow are measured with sensors listed in table 1. Turbine mass flow is the sum of fuel flow and intake air flow (MAF sensor). In order to avoid the introduction of errors in the mass flow measurements, the exhaust gas recirculation (EGR) valve is completely closed. Water-cooled pressure transducers sampling at 0.1 engine crank angle degrees (CAD) intervals up to 500 kHz are positioned at the turbine connection to the exhaust manifold and at the turbine outlet. Moreover, temperature of exhaust gasses before entering the turbine is measured through a 3 mm k-type

thermocouple. In the case of turbine outlet temperature, eight thermocouples at different depths are placed in a straight insulated duct in order to convey with the presence of swirling flows [10].

2.2 Unsteady performance measurements

It has been shown that the engine gas-stand can allow performance measurement of turbochargers [10]. On the compressor side, flow pulsations are only caused by oscillating speed of the turbocharger shaft, induced by turbine inlet variable unsteady conditions. Therefore, time-average data are able to represent the instantaneous conditions of compressors, as it is operating under quasi-steady conditions. Moreover, as also observed in other research papers [1, 9], the engine gas-stand allows investigation of turbine inlet temperature (TIT) influence on apparent efficiencies. A high temperature at the turbine inlet causes the apparent compressor efficiency at low mass flow to drop as heat is transferred to the compressor housing. In this scenario, the compressor outlet temperature increases, lowering the overall efficiency of the compressor stage.

As well as the compressor, turbine performance can be monitored in the engine gas-stand. In order to measure turbine performance for an automotive turbocharger, data available from the experimental test rig are exploited. Due to the presence of unsteady flow in the exhaust, the sampling frequency of pressure, temperature and mass flow sensors has a significant importance. In fact, in case of two different acquisition rates, measurements to define swallowing capacity of the turbine could differ. In this study, two acquisition frequencies for pressure transducers have been adopted, as low as 1 Hz for the 'slow' sampling case (minimum sampling frequency for fuel metering system) and 120 kHz at 'fast' sampling conditions (maximum sampling frequency achievable at engine speed of 2000 rpm), depending on engine speed. Temperature and mass flow measurements have been monitored at 1 Hz under 'slow' and 'fast' sampling rates. In addition, turbine swallowing capacity has been investigated at 0.5 VGT position, having

pulsating flows at the turbine inlet at a frequency of 66.67 Hz. It could be suggested that the acquisition rates would not be adequate to capture the effects of oscillating flows on temperature, mass rates and pressure, in the case of 'slow' sampling speed. In fact, it is suggested that aliasing distortion [30] could be encountered in the experimental data, apart from 'fast' sampled pressure.

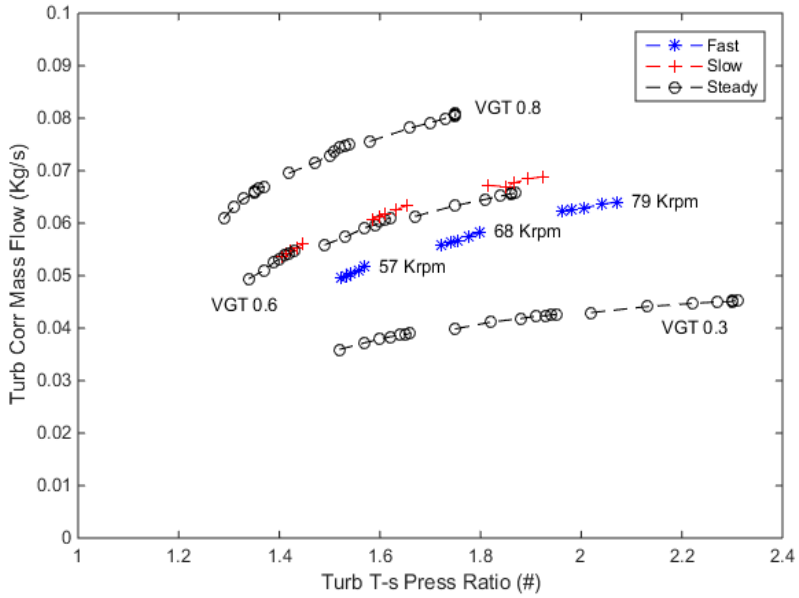

Figure 2. Experimental 0.5 VGT turbine performance data acquired at 'slow' and 'fast' sampling speeds and compared to steady turbocharger manufacturer's data available at 0.3, 0.6 and 0.8 VGT opening positions. 'Fast' sampled data are cycle averaged. 'Slow' sampled data are averaged for 60 sec. VGT has a travel of about 50 mm between 0 and 1 positions.

In figure 2, points from the steady manufacturer's map at 0.3, 0.6 and 0.8 opening positions of the variable geometry turbine (VGT) are shown. These data are compared to turbine performance measured in the engine gas-stand using 'fast' and 'slow' acquisition speeds. Although, the difference in the VGT opening position, 'slow' measured turbine swallowing

capacities for three corrected speed lines at 57, 68 and 79 Krpm (actual turbocharger speeds of 99, 118 and 138Krpm) are similar to steady performance map data at 0.6 VGT. This similarity is certainly dismissed once pressure events on a higher frequency spectrum are analysed in the 'fast' acquisition case. In fact, 'slow' acquisitions at 1Hz are only able to measure once per second with the pressure recorded being anywhere between minimum and maximum values of peaks in the 66.67 Hz oscillating trace. In conjunction with figure 3.19, this results in an underestimation of turbine pressure ratio and overestimation of corrected turbine mass flow, depending also on turbine inlet pressure. However, in the engine gas-stand, the impossibility to improve sampling rates of temperature and mass flow thus omits the dynamic effects of the exhaust process, occurring at 66.67 Hz in the experimental setting. It is clear that a lower acquisition rate of pressures at the turbine would not be adequate enough in the representation of the real performance. In fact, the averaging of pressure measurements at elevated sampling frequency shows a different pressure ratio.

2.3 Effect of turbine inlet temperature

The obtained improvement in increasing sampling frequencies has led to calculation of T-s turbine efficiency considering values for the 'fast' acquisition, due to improvement over aliasing distortion of measurements [30]. Due to temperature dependency of turbine performance, measurements have been monitored through 3mm k-type thermocouple at turbine inlet and 1.5mm k-type thermocouple at turbine outlet. Unfortunately, the thermocouples adopted in the engine gas-stand are characterised by a significantly low response rate and a possible increment over the 1Hz sampling rate would not have been beneficial. Although, inaccuracy of temperature measurements owing to the presence of oscillating flows, further errors could be introduced because of the thermocouple position since only average temperatures could be obtained

experimentally. For this reason, two identical thermocouples have been placed at different locations in the exhaust and turbine inlet sections, shown in figure 3, and turbine measurements have been performed for operating conditions shown in figure 4.

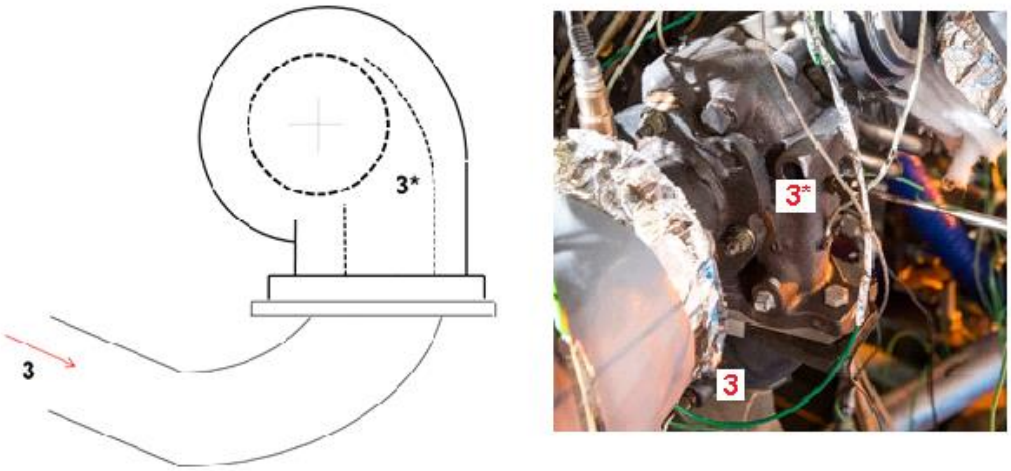

Figure 3. Schematic of the two thermocouple at 3 and 3* for the evaluation of TIT

In figure 3, flow temperature has been monitored at the exhaust manifold exit (i.e. inlet to the turbine) (3) and at the turbine tongue (3*). The outlet temperature at 4 has been considered as a unique average value of the thermocouples as plotted in figure 4. Therefore, T-s turbine efficiency could be calculated for the two different TIT indicated. It could be expected that the flow temperature in the proximity of the turbine would be lower due to heat transfer in the exhaust section. However, the analysis highlights that higher efficiency could be measured, referencing 3* as TIT. In this scenario, measurements suggest that conditions at 3* are hotter than the thermocouple in 3.

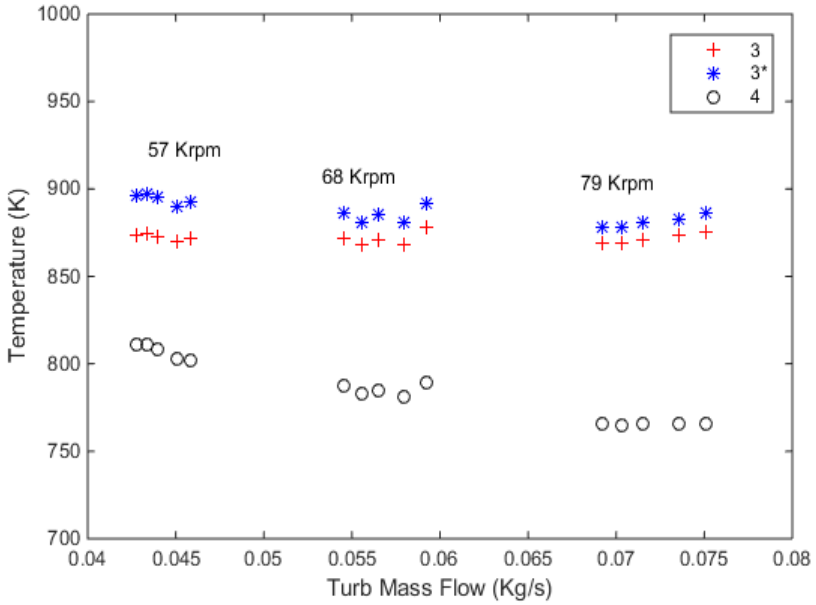

Figure 4. Turbine mass flow and experimental temperatures measured in the engine gas-stand at the positions 3 (turbine inlet temperature), 3* (turbine inlet temperature in the turbine tongue and in the proximity of the turbine rotor) and 4 (turbine outlet temperature averaged across eight thermocouples) for the three corrected speed lines at 57, 68 and 79 krpm

The cause for higher time-average temperature at the proximity of the turbine rotor could be given by the possibility of exhaust gasses to converge towards the turbine rotor. The thermocouple closer to the turbine tongue (3*) would be measuring temperature under different conditions of the thermocouple positioned at 3. In fact, it would seem that the thermocouple positioned at the exhaust manifold (position 3) is affected by 3D temperature distribution, due to the close proximity of multiple Y-junctions and bends in the exhaust manifold. In this scenario, the temperature at the tip of the thermocouple 3* would be similar to a 1D flow domain. However, a 3D flow analysis would be required to improve the understanding, as investigated in [20].

Furthermore, the reduction of diameter at the turbine inlet towards the turbine tongue and volute would accelerate the flow velocity. Accordingly to the definitions of Strouhal number and reduced frequency, it would result in a reduction of the flow unsteadiness.

3. Hybrid unsteady/quasi-steady turbine model

3.1 Modelling approaches

In order to represent turbochargers performance in 1D powertrain models, steady performance maps for compressor and turbine are adopted, assuming that the turbocharger behaves quasi-steadily. In the case of a turbine, boundaries at inlet and outlet of the turbomachine are coupled to the performance maps, replacing internal volumes from tongue to diffuser. Additionally, in internal combustion engines application, TIT and turbine outlet temperature (TOT) are measured at exhaust manifold exit and at exhaust duct preceding after-treatment systems, respectively. In 1D powertrain model simulations, average temperature is monitored via virtual sensors for the considered radial section of the duct. In this research study, virtual temperature sensors (VTS) and thermocouple (VTC) models have been positioned at 3, 3* and 4 to evaluate TIT and TOT and account for the predicted turbine performance. Moreover, two turbine models have been implemented and temperature measurements through virtual sensors and thermocouples have been evaluated, in order to improve efficiency and TOT representation. In particular, five modelling approaches have been developed as shown in table 2, specifying turbine and temperature models. Furthermore, in the five modelling approaches, pressures at turbine inlet and outlet are monitored in the same location as in the experimental tests.

Table 2. Modelling approaches of turbine in an automotive turbocharger

	Turbine Model	Turbine inlet and outlet	TIT	TOT
Virtual T3	Steady Map	In turbine map	VTS 3	VTS 4
Virtual TC3	Steady Map	In turbine map	VTC 3	VTC 4
Virtual T3*	Hybrid unsteady/quasi-steady	Tapered ducts	VTS 3*	VTS 4
Virtual TC3*	Hybrid unsteady/quasi-steady	Tapered ducts	VTC 3*	VTC 4
Virtual TC3*-T4	Hybrid unsteady/quasi-steady	Tapered ducts	VTC 3*	VTS 4

In the case of virtual T3 and TC3, steady maps for the entire turbine have been considered. In order to account for the temperature at 3*, the hybrid unsteady/quasi-steady turbine model has been developed. The model differs from the approach adopted by Piscaglia et al. [22], because of the adoption of tapered ducts at the turbine inlet and diffuser, instead of volumes for mass storage behaviours. In addition, in the hybrid unsteady/quasi-steady turbine model, turbine volute is modelled in the steady turbine map, in order to account for part of the expansion process taking place upstream the turbine rotor. On the other side, both models from Piscaglia et al. [22] and Chiong et al. [23] are modelling turbine volute in volumes and ducts, respectively. As suggested by Yang et al. [31], in the duct between the turbine inlet and the tongue (inlet of the volute), the phase shift in pressure and temperature is significantly noticeable. In addition, this phase shift is highly reduced along the volute, due to the increased bulk flow velocity. In fact, the increase in flow velocity can be supported by the reduction of the cross sectional area. It is

important to notice that the increase of flow velocity is inversely proportional to the flow unsteadiness, as supported by the Strouhal number [32] and the reduced frequency [33].

In the hybrid unsteady/quasi-steady turbine model, turbine tongue and diffuser are treated as unsteady, being modelled though tapered ducts, while the unscaled turbine steady performance map represents the expansion process in the rotor. Unlikely, in the hybrid unsteady/quasi-steady turbine model, frequency tuning is not necessary as the steady turbine map is adopted for the expansion process, considering volute and rotor operating under quasi-steady conditions. This representation can be valid for small volutes and steady turbine maps can be adopted for the quasi-steady expansion process, allowing simultaneously the monitoring of TIT closer to the turbine rotor. The proposed hybrid unsteady/quasi-steady turbine model would be able to represent the unsteady flow operations of turbine inlet (up to the turbine tongue) and turbine diffuser. Due to the difficulty in obtaining geometrical data from turbochargers, the turbine model has based the dimensions of added unsteady flow sections to the model from simple real geometrical measurements. In addition, no further tuning to represent steady and unsteady flow conditions has been applied. Furthermore, non-intrusive measurements can be performed without dismantling the turbomachine to evaluate turbine tongue and diffuser dimensions. A diagram of the 1D hybrid unsteady/quasi-steady turbine model can be visualised in figure 5. The turbine inlet to the tongue is modelled as a 78.65mm tapered duct, with diameters of 34mm at the inlet and 25mm (turbine tongue side) at the outlet. Meanwhile, the turbine outlet is modelled as a 40mm tapered duct, with diameters at the inlet of 44mm (turbine wheel side) and 60mm at the outlet.

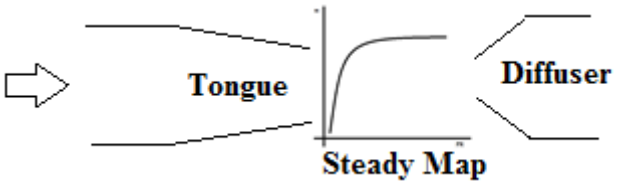

Figure 5. Hybrid unsteady/quasi-steady turbine model

Referring to table 2, the hybrid unsteady/quasi-steady turbine model is adopted in three simulation approaches, as virtual T3*, virtual TC3* and virtual TC3*-T4. In these 1D models, TIT is correlated to thermocouple measurements at the turbine tongue in the experimental engine gas-stand. As visible, TIT and TOT are modelled through virtual temperature sensors (VTS), evaluating the temperature at a section of the duct, and virtual thermocouples (VTC), considering the thermal characteristics of the mineral insulated k-type thermocouple. In the latter case, a grounded thermocouple with wires diameter of 0.3 mm has been defined, solving the governing heat transfer equations of appendix A. The 3 mm 304 stainless steel sheath is modelled with a thickness of 0.5 mm. In addition, the thermocouple tip is position within the turbine tongue flow, approximately, at the centre of the duct. Specifically, in the hybrid unsteady/quasi-steady turbine model, the turbine inlet has the dimension of a tapered duct with inlet and outlet diameters of 34 mm and 25 mm, respectively. The total length of the turbine inlet up to the tongue consists of 78.6 mm which has been externally measured from the experimental turbocharger turbine tested in the engine gas-stand. The VTC is positioned 74.5 mm away from the inlet of the turbine tongue. Furthermore, the turbine diffuser is represented as a 40 mm long tapered duct with inlet and outlet diameters of 44 mm and 60 mm, respectively.

3.2 Models calibration procedure

In the engine gas-stand, compressor outlet is not connected to engine intake and there is not direct influence. In order to calibrate the 1D powertrain model, intake and exhaust conditions of the engine have to correspond to the experimental data. Therefore, engine inlet conditions can be targeted defining the correct boundaries as provided by the boost rig. In order to correlate exhaust and turbine operations, the VGT position has been imposed at 0.5, in agreement with the

experiments. Moreover, mass flow through the system is achieved by targeting air and fuel flows. A correlation of modelled combustion events with experiments would generate correct exhaust flow temperature. In this scenario, heat transfer characteristics of exhaust manifolds and ducts have been defined in connection with the materials.

In order to reduce the gap between experimental and modelled temperature estimates, heat transfer multipliers for exhaust ducts, including turbine tongue and diffuser for the hybrid unsteady/quasi-steady model, have been increased. Under these circumstances, an absolute error in TIT prediction of 10 K has been targeted using a unique heat transfer multiplier for each of the three corrected turbine speed lines (57, 68 and 79 krpm). On the other side, heat transfer multiplier for turbine diffuser has been defined equal to turbine inlet and exhaust manifold settings. Furthermore, it is important to consider that the turbocharger has been subjected to acceleration/deceleration in relation to the measured inertia of the shaft. In this way, the instantaneous acceleration/deceleration of the turbine rotor is considered in the instantaneous variation of turbocharger power [32, 34].

4. Results and discussion

4.1 Average data correlation

In order to quantify possible benefits from the adoption of the novel unsteady/quasi-steady turbine model into the 1D engine gas-stand simulation, performance parameters related to the turbine have been investigated for the 15 operating conditions tested in the engine gas-stand facility. Therefore, turbocharger speed, turbine mass flow, turbine inlet and outlet pressures and TOT are evaluated for correlation between experiments and simulation results. Specifically, in this section, time-average values are compared and analysed in relation to the 1D predictions presented. It is important to notice that 1D modelled time-average terms are matched for sampling frequency to

the experimental acquisition equipment in the experimental engine gas-stand facility. In particular, in order to assess the correlation between predicted and measured conditions of the air-path and turbine operations, time-average simulation results have been investigated at 1Hz for TOT and turbine mass flow. Due to the higher sampling rate in the experimental facility, turbocharger speed and turbine inlet and outlet pressures have been analysed at intervals of 0.1CAD, resulting in 120KHz at an engine speed of 2000rpm. From figure 6 to 10, prediction differences relative to the experimental measurements are presented. Steady turbine map (T3 and TC3) and hybrid unsteady/quasi-steady (T3*, TC3* and TC3*-T4) turbine models are compared for several turbocharger operating conditions.

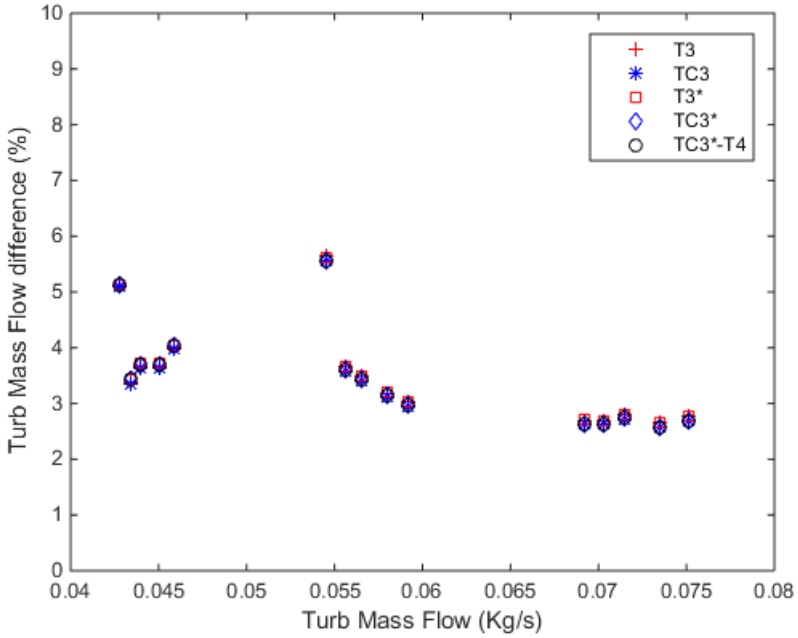

Figure 6: Difference between predicted turbine mass flow and experimental turbine mass flow measured in the engine gas-stand

In figure 6, the maximum difference in predicted turbine mass flow consists of about 6%. It is important to notice that the differences remain similar for the several turbine modelling approaches under the same operating condition. Although, in the hybrid unsteady/quasi-steady turbine model, turbine inlet until the tongue and diffuser are modelled as converging and diverging ducts, respectively, this seems to have a reduced effect on the engine back-pressure. However, the predicted turbine mass flow remains unaffected from the variation in turbine modelling approaches. Moreover, slightly different results have been recorded in the turbocharger speed prediction, shown in figure 7. Turbocharger speed differences in the modelling approaches are visualised against turbine mass flow, instead of absolute turbocharger speeds, in order to identify a possible mass flow dependency. In this figure, the highest difference value of about 10% is found at the largest turbine mass flow for the TC3*-T4 and TC3* models. In both these scenarios, the hybrid unsteady/quasi-steady turbine model is implemented, suggesting an over-prediction of turbine expansion ratio. Therefore, the novel turbine model suggests that a slightly higher back-pressure can be caused due to the increasing predicted turbocharger speed compared to steady turbine map alone. The slight rise of difference in turbocharger speed prediction at high turbine mass flow could be supported, due to the limited number of experimental data points populating the steady turbine map at 79Krpm, meaning that turbine performance are based on extrapolated data points.

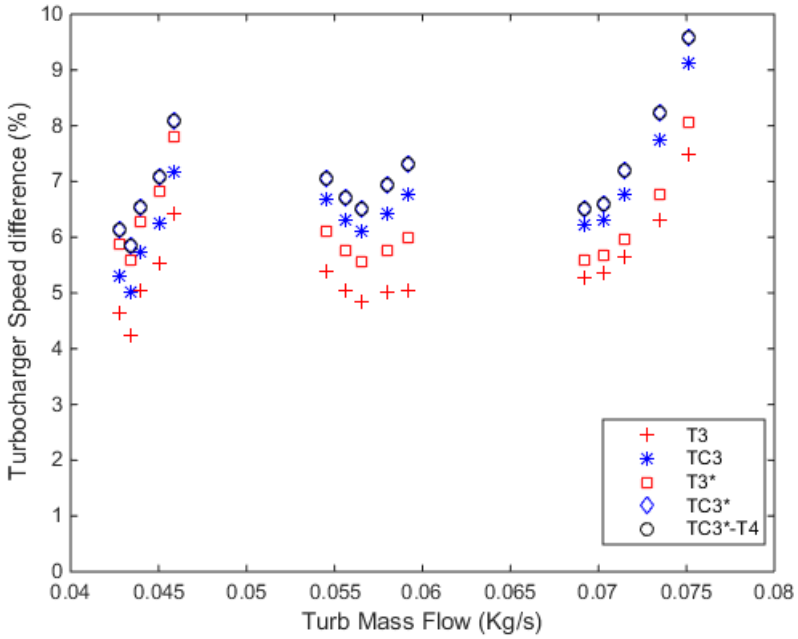

Figure 7: Difference between predicted turbocharger speed and experimental turbine mass flow

Figures 8 and 9 confirm the increase of back-pressure through the implementation of the hybrid unsteady/quasi-steady turbine model. Although, the maximum difference is of about 12% and 10% for inlet and outlet pressures, respectively, gap between experimental and simulated values is maintained similar at inlet and outlet of the turbine. It is important to state that the pressure measurements in the engine gas-stand are able to consider the different pressure peaks, in correlation to the exhaust discharge events of every cylinder. In addition, the measurement of static pressure in the exhaust manifold is able to capture the 3D pressure distribution inside the exhaust manifold. These phenomena are not represented into the 1D model simulation and a possible difference of predicted turbine inlet and outlet pressures from the experimental data can occur. In figures 8 and 9, differences in predicted turbine inlet and outlet pressures are displayed against the absolute experimental pressure values, respectively. Additionally, in T3*, TC3* and

TC3*-T4 modelling approaches, the positive error recorded in figure 8 is resembled at the turbine outlet pressure of figure 9. In this way, the novel turbine model would be able to maintain the prediction over turbine pressure ratio. However, a scaling of turbine diameter might be required due to the restricted dimension across the turbine rotor. Overall, differences for predicted turbine inlet and outlet pressures in steady turbine maps show a maximum difference of about 5% between predicted and experimental values in figures 8 and 9.

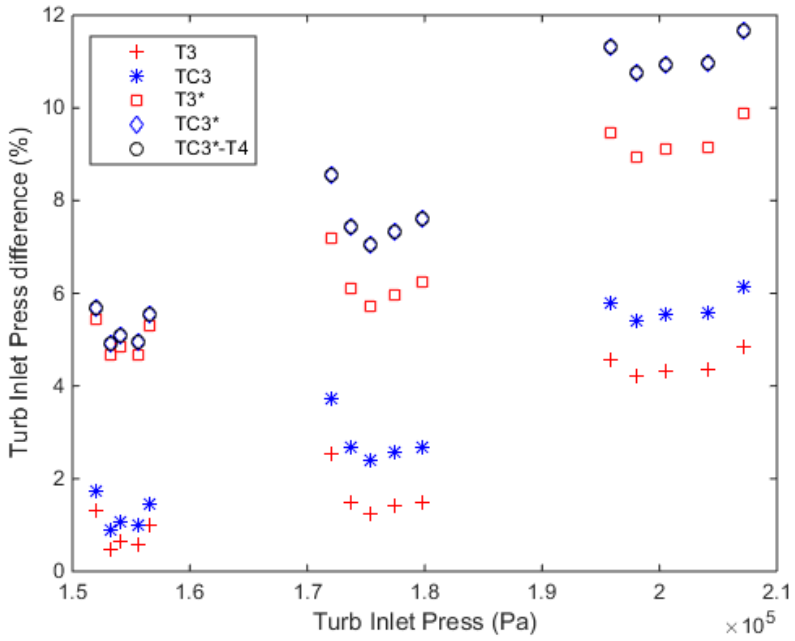

Figure 8: Difference between predicted turbine inlet pressure and experimental turbine inlet pressure

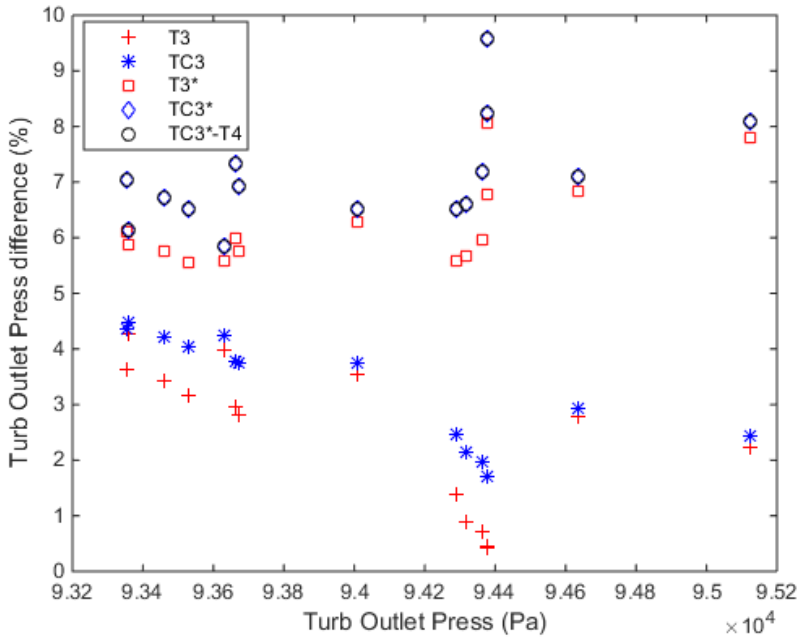

Figure 9: Difference between predicted turbine outlet pressure and experimental turbine outlet pressure

The investigation of estimated average outlet temperature correlates to the experimental values with different precision, accordingly to the turbine modelling method. Steady turbine maps cause an over-prediction of turbine outlet temperature as a minimum of 20K, as supported by figure 10. The implementation of the hybrid turbine model is able to reduce the gap between experimental and modelled TOT, for virtual sensors included at inlet and outlet turbine flows. However, the assumption of equivalency between the average TIT across a radial section of the modelled duct and the temperature measured through a thermocouple in the engine gas-stand is not recommended. Therefore, the use of virtual thermocouple at 3* and virtual sensor at 4 would refer to the type of instrumentation adopted in the experimental rig, as best represented by a maximum difference of about 25K in TOT prediction through the TC3*-T4 model of figure 10. It is important

to highlight that sampling frequency of predicted and measured temperatures have been matched for comparison. In fact, a frequency of 1Hz has been chosen, due to the limits in reaction time of real thermocouples in the engine gas-stand.

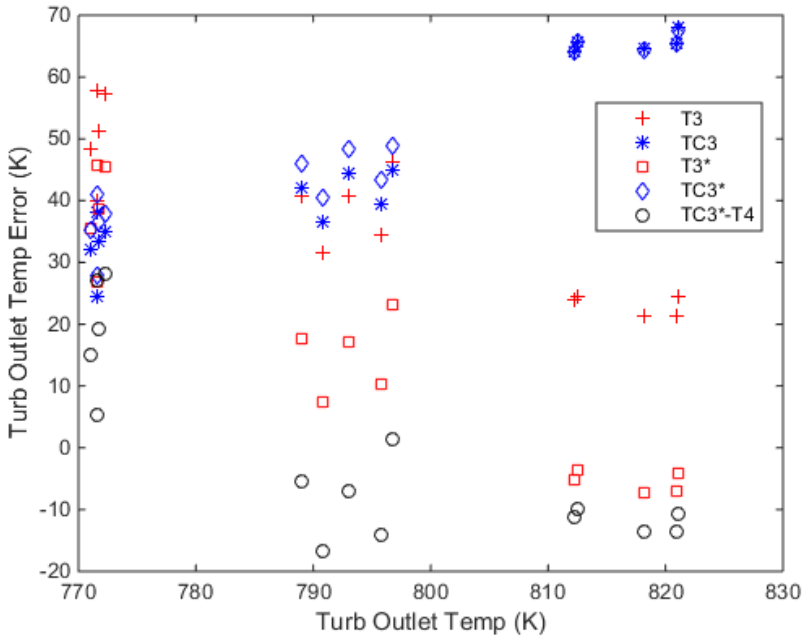

Figure 10: Temperature difference between experimental and predicted TOT against experimental TOT values

4.2 Instantaneous turbine performance correlation

From the experimental data available in figure 4, the modelling approaches of table 2 have been applied to the 15 operating conditions of the turbine, including steady map and hybrid unsteady/quasi-steady turbine representations. As well as evaluating the proposed turbine model under time-averaging at fixed sampling frequencies, instantaneous measurements would be able to provide additional details, focussing on the improvement of turbine performance representation. In fact, through an accurate analysis, instantaneous temperature and pressure

correlations between experiments and simulations can be investigated. In this scenario, in order to quantify qualities of the proposed turbine modelling method, one operating condition of the turbocharger turbines has been investigated for instantaneous performance evaluation. According to time-average data, attention has been focused on pressure ratio, turbine total-to-static efficiency and turbine inlet and outlet temperatures.

Therefore, turbine performance for one operating condition at corrected turbine speed of 79 krpm are exploited to evaluate improvements over representation of turbine performance in the 1D model. This operating speed has been considered due to the maximum discrepancy recorded between predicted and measured turbine inlet and outlet pressures, shown in figures 11 and 12. In fact, although, these magnitude of errors refer to average pressure values, the highest change in turbine performance between prediction and experiments is expected. Additionally, T-s turbine efficiency has been calculated using virtual thermocouples, reflecting the thermal behaviour of the sensing material, and virtual temperature sensors, evaluating the temperature of the flow for a section of the duct.

Table 3. Correlation of turbine performance for steady map approaches

	PR	**Mass Flow**	**Speed**	$\eta_{T\text{-}s}$
Experimental 3	2.08	0.0692 kg/s	79 krpm	0.68
Virtual T3	-0.5%	+2.6%	+5.3%	-8.8%
Virtual TC3	+0.5%	+2.6%	+6.2%	+19.1%

Table 4. Correlation of turbine performance for hybrid unsteady/quasi-steady approaches

	PR	**Mass Flow**	**Speed**	**η_{T-s}**
Experimental 3*	2.08	0.0692 kg/s	79 krpm	0.73
Virtual T3*	0%	+2.6%	+5.6%	-9.6%
Virtual TC3*	+1%	+2.6%	+6.5%	+24.6%
Virtual TC3*-T4	+1%	+2.6%	+6.5%	-20.5%

In tables 3 and 4, pressure ratio (PR), turbine mass flow, turbocharger speed and T-s turbine efficiency (η_{T-s}) related to experiments and simulations are reported. It is important to consider that the average efficiency is dependant of instantaneous pressure and temperature trends. The predictions from tables 3 and 4 refer to engine cycle-average calculations considering the sampling frequency for each of the variables monitored in the experiments. The efficiency calculated in the experimental gas-stand has been calculated from instantaneous pressure and temperature. Although, the former could be directly measured in the engine gas-stand, the latter has been generated by the implementation of equation 1. Therefore, a polytropic process has been assumed in the engine exhaust, where ratio of specific heats (γ) are depending on the engine AFR and the combustion products, i.e. CO_2, water vapour, nitrogen and oxygen in excess. Moreover, the cycle-averaged efficiency could be calculated. In relation to the experimental values, instantaneous temperatures (T_{inst}) have been computed through instantaneous (P_{inst}) and average (P_{ave}) pressure and temperature (T_{ave}) information in equation 1, in conjunction with the ratio of specific heats (γ) of the polytropic process[32].

$$T_{inst} = T_{ave} * \left(\frac{P_{inst}}{P_{ave}}\right)^{\frac{\gamma-1}{\gamma}} \quad (1)$$

In addition, the predicted turbine efficiency in the models has been generated in a similar way to the experimental calculated efficiency. Due to the possibility to monitor instantaneous temperatures in the1D model, equation 1 has not been applied to the predicted temperatures in models. In this way, the comparison between simulations and experiments could be maintained reasonable. Analysing the average data information in tables 3 and 4, it seems that the virtual T3 model, adopting the turbine steady map approach and virtual sensors for temperature estimation would be able to represent engine gas-stand performance better than other approaches. Although, the matching of average turbine performance is important to state the validity of the model, investigation of instantaneous sensors data would show a change in prediction. In figure 11, the experimental pressure ratio from the engine gas-stand is compared with the simulations. However, in figure, discrepancies could be noticed in the peaks, reaching about 12% of differences in the prediction of pressure ratio. Moreover, the structure of the experimental rig allowed positioning of pressure transducers in the proximity of position 3 and 4.

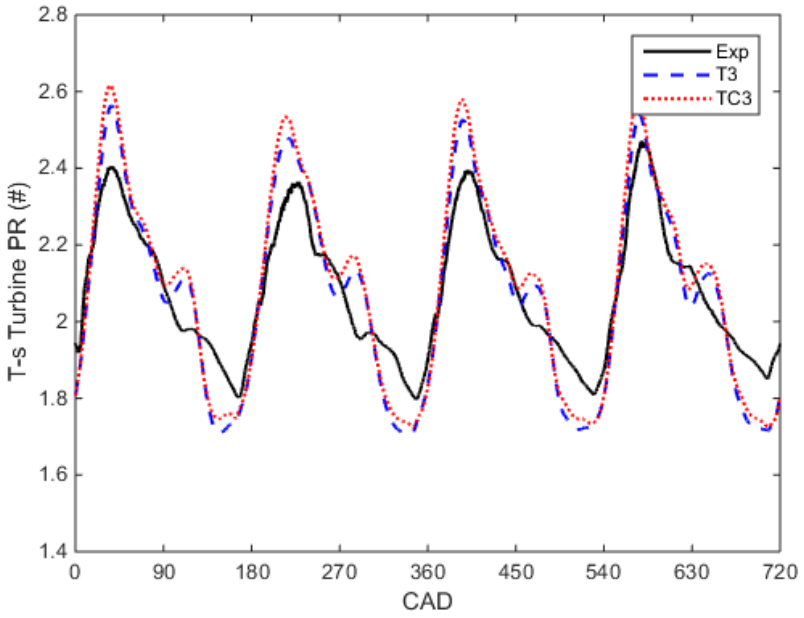

Figure 11. Instantaneous PR from experimental (3) and modelled (T3 and TC3) analyses of the same turbine operating condition

Most importantly, the TIT has been analysed in figure 12, showing that T3, TC3, T3* and TC3* in comparison to instantaneous data of experimental temperatures, assuming a polytropic process, at 3 and 3*. In equation 1, experimental temperature at 3* includes instantaneous pressure solely at position 3, as the available pressure transducer at turbine inlet. It seems than the hybrid model of the turbine can allow an improvement, correlating experimental and modelled TIT. In fact, it is important to notice that thermocouples for turbine inlet flow measurements are able to capture average temperature, due to low rate of response. The adoption of the virtual thermocouple is not able to show a particular difference towards virtual sensors, apart from slower response to temperature reductions. Moreover, experimental T-s turbine efficiency has lower rate of oscillation compared to simulated approaches as shown in figure 13. This scenario can be

explained by significant difference between experimental and modelled instantaneous TIT. In fact, a lower amplitude of fluctuation is recorded in the experimental temperatures of figure 12. In relation to the virtual temperatures, it appears that T3 and TC3 approaches recorded significantly higher fluctuations compared to T3* and TC3*. Therefore, the adoption of 1D hybrid unsteady/quasi-steady turbine model can reduce the gap with experiments, on the basis of the obtained instantaneous temperatures obtained by equation 1.

Furthermore, it is important to notice that the resulting pressure and temperature predictions are related to the discretisation length adopted. In the 1D models, suggested discretisation length of 30mm is adopted. Moreover, heat capacities representing the exhaust manifold mass are neglected, although these are expected to have a significant role towards the modelling of the flow temperature. Therefore, a reduction of the temperature slope would be achieved with the inclusion of heat capacities.

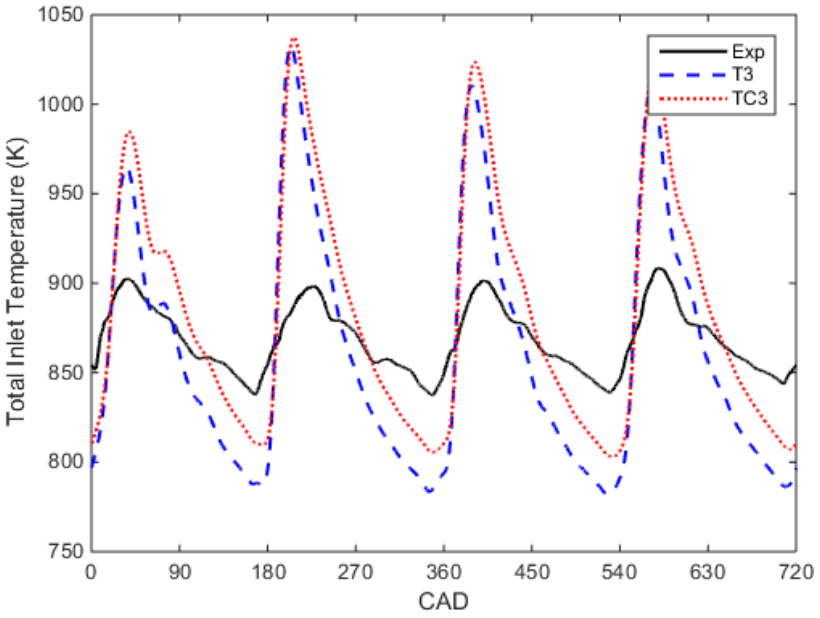
Exp
T3
TC3
Total Inlet Temperature (K)
CAD
1050
1000
950
900
850
800
750
0
90
180
270
360
450
540
630
720

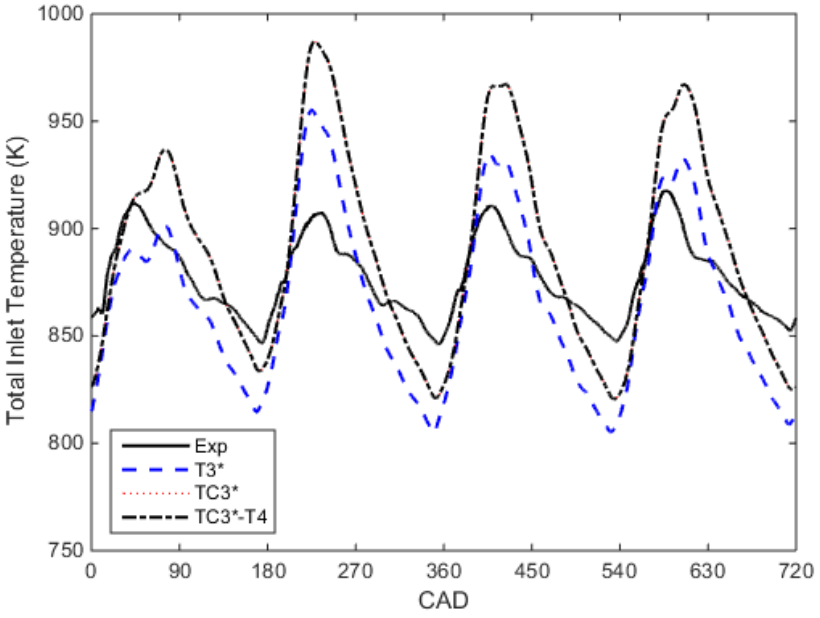
Exp
T3*
TC3*
TC3*-T4
Total Inlet Temperature (K)
CAD
1000
950
900
850
800
750
0
90
180
270
360
450
540
630
720

Figure 12. Instantaneous total TIT from experimental (3 and 3*) and modelled (T3, TC3, T3* and TC3*) analyses of the same turbine operating condition. Experimental values of temperatures are calculated using equation 1.

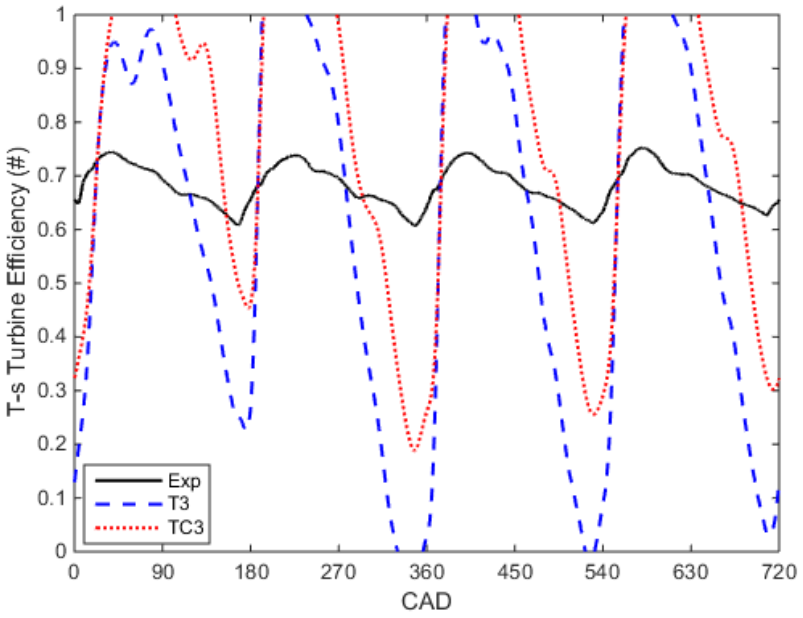
T-s Turbine Efficiency (#)
CAD
Exp
T3
TC3
0
0.1
0.2
0.3
0.4
0.5
0.6
0.7
0.8
0.9
1
0
90
180
270
360
450
540
630
720

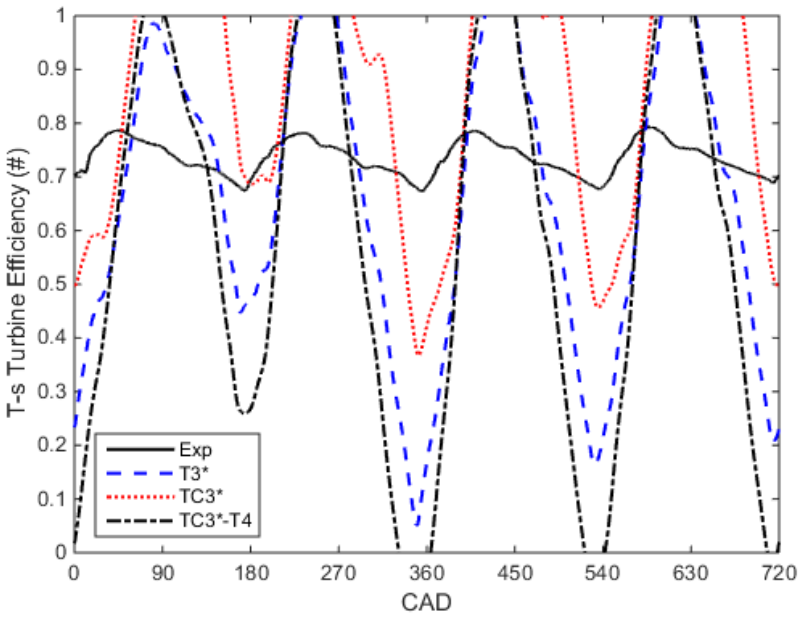
T-s Turbine Efficiency (#)
CAD
Exp
T3*
TC3*
TC3*-T4
0
0.1
0.2
0.3
0.4
0.5
0.6
0.7
0.8
0.9
1
0
90
180
270
360
450
540
630
720

Figure 13. Instantaneous T-s turbine efficiency from experimental (3 and 3*) and modelled (T3, TC3, T3* and TC3*) analyses of the same turbine operating condition. Experimental values of temperatures are calculated using equation 1.

In addition, a similar trend is present once the instantaneous measurements are included for the calculation of total-to-static turbine efficiency, as plotted in figure 13. It is important to understand that the modelled efficiencies of figure 13 are evaluated by the implementation of predicted instantaneous temperature in the total-to-static efficiency formula (equation 1). In fact, due to the larger predicted temperature fluctuations of figure 12, impossible efficiencies higher than 100% are recorded. Moreover, it is important to understand that the heat transfer in ducts between temperature measurements and turbine rotor are modelled, in order to resemble the experimental setting. In order to evaluate the prediction, the maximum amplitude of oscillation in the efficiencies of figure 13 is reported in tables 5 and 6. As suggested, a reduced fluctuation is predicted through the virtual TC3* approach resulting in an efficiency amplitude of 0.97. Comparing approaches, it is evident that lower fluctuations are achieved with virtual thermocouple models due to representation of the physical element and the additional thermal masses of a mineral insulated k-type thermocouple. However, in the case of virtual thermocouples at turbine inlet and virtual temperature sensor at turbine outlet, in TC3*-T4, an elevated oscillation in turbine efficiency is recorded compared to the experimental conditions.

Table 5. Efficiency amplitude for steady map approaches

	Efficiency amplitude
Experimental 3	0.14
Virtual T3	1.39
Virtual TC3	1.07

Table 6. Efficiency amplitude for hybrid unsteady/quasi-steady approaches

	Efficiency amplitude
Experimental 3*	0.11
Virtual T3*	1.02
Virtual TC3*	0.97
Virtual TC3*-T4	1.27

As well as TIT, the analysis of TOT would be able to validate the turbine models in the prediction of turbine efficiency. Total outlet temperatures are significantly reduced through the turbine, as visible in figure 14. However, the experiments suggest that the instantaneous temperature is stable across the engine cycle, due to steady turbine outlet pressure. Furthermore, it is important to notice that thermocouples have been adopted for capturing exhaust flow temperature in the TC3 and TC3* simulations. These have resulted in a slightly lower temperature than measurements through virtual sensors as supported by figure 14. In addition, several thermocouples have been used in the experimental engine gas-stand facility, due to marked flow motion at the turbine outlet. In order to evaluate the instantaneous temperature using equation 1, the average temperature of the multiple thermocouples at the exhaust has been introduced into

the equation as T_{ave}. In this scenario, a virtual sensor averaging the temperature across a radial section of the duct would be able to reflect the experimental values.

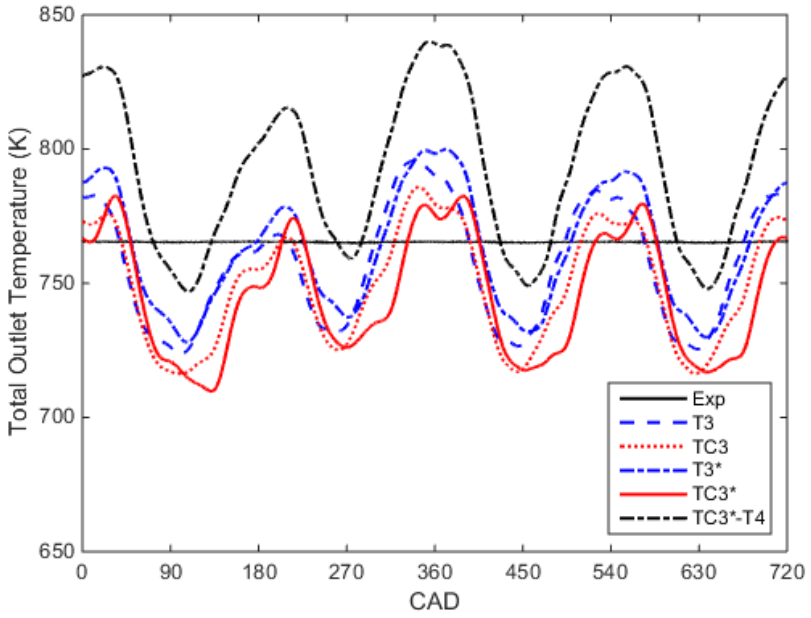

Figure 14. Instantaneous TOT from experimental (T4) and modelled (T3, TC3, T3* and TC3*) analyses of the same turbine operating condition. Experimental values of temperatures are calculated using equation 1.

5. Conclusions

The development of a turbine model to account for unsteady conditions in the engine gas-stand is presented. The main conclusions can be listed below:

- Modelling of turbine tongue for 1D flow simulations have shown that a closer matching between the time-average experimental turbine inlet temperature and

the virtual temperature is possible. In fact, the converging dimensions at 3* cause a reduction of temperature oscillation, as supported by simulations, increasing fidelity in TIT correlation.

- Moreover, the use of virtual temperature sensors in T3* model is beneficial in the representation of TIT at 3*, as supported by the temperature gap for the average TOT. However, this is valid when TOT is correlated with virtual temperature sensors which could represent the measured temperature across a radial section of the exhaust duct.
- The hybrid unsteady/quasi-steady turbine modelling approach has not been combined with heat transfer correction factors, limiting the adoption of the model to medium/high turbocharger speeds where heat transfer has reduced impact on the turbine gas flow temperature.
- Furthermore, the adoption of experimental steady turbine performance maps marks the dependency of the model accuracy on the number of data points available. In fact, a significant difference increase regarding predicted turbocharger speed could be recorded as at high mass flow values in figure 7.
- The proposed turbine model has showed an attempt to include the unsteady flow behaviour, although, higher degree of information would be required, in order to optimise the approach, such as the VGT internal opening areas. However, the use of 3* temperature could be applied as a reference for two-stage turbocharging systems, reducing the effect of heat transfer in ducts.

Acknowledgement

The Authors would like to acknowledge the technical staff at the Powertrain and Vehicle Research Centre for the support received in implementing the experimental facility. The Authors would like to acknowledge the University of Bath and the Institution of Mechanical Engineers for the financial support to facilitate the collaboration between the University of Bath and NTU.

Appendix A

A.1 Thermocouple model and heat transfer equations

The thermocouple model adopted in the 1D powertrain model considers heat transfer from the flow to the sensing elements. Due to the presence of an insulating heat sheath in the thermocouple, equations for conduction, convection and radiation are solved, in order to calculate the temperature sensed by the thermocouple bulb and wire. According to the plot in figure A.1, heat is transferred through convection from the hot gas flow to the thermocouple sheath. In the case of an insulated and grounded thermocouple, the heat is radiated and conducted to the surrounding walls. Meanwhile, the remaining heat is sensed by the thermocouple through the bulb. Therefore, it is clear that part of the heat contained in the gas flow is not being sensed by the thermocouple bulb.

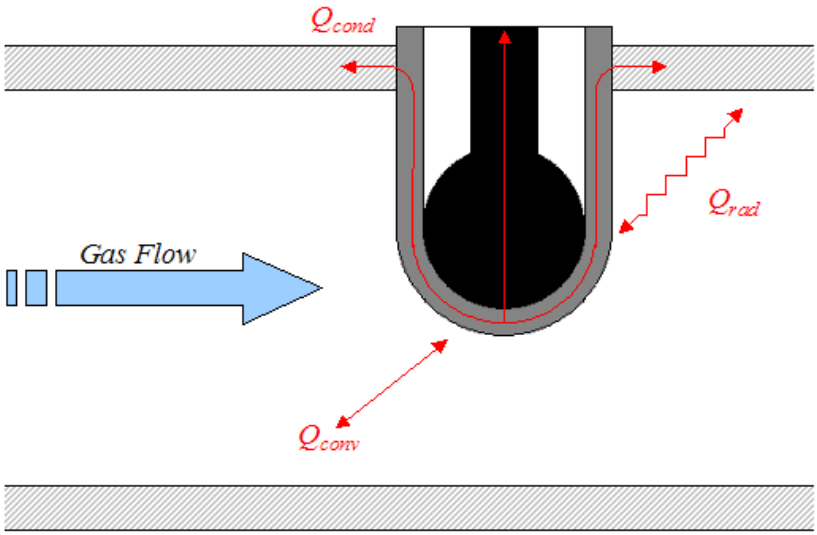

Figure A.1. Thermocouple model as represented in the 1D model developed in Ricardo WAVE®

Specifically, equation for heat exchanged through convection (Q_{conv}) and radiation (Q_{rad}) are solved as in equations A.1 and A.2.

$$Q_{conv} = hA_{tip}(T_{gas} - T_{tip}) \quad \text{(A.1)}$$

$$Q_{rad} = \varepsilon\sigma F A_{tip}(T_{wall}^4 - T_{tip}^4) \quad \text{(A.2)}$$

In this case, temperature of the gas (T_{gas}), thermocouple tip (T_{tip}) and duct wall (T_{wall}) are required in order to estimate the heat being captured by the sensing element of the thermocouple. Furthermore, it is important to consider the convective heat transfer coefficient (h) of the various

thermocouple elements, such as the sheath, the bulb and the wire. Lastly, the definitions of the terms in the equations are reported in the table A.1.

Table A.1. Definitions of the terms in equations A.1 and A.2

h	Convective heat transfer coefficient [W/m2/K]
A	Area [m2]
T	Temperature [K]
ε	Emissivity (0.8)
σ	Stefan-Boltzman constant (5.669e-08 [W/m2/K4]
F	Radiation View factor to walls (1.0)

Appendix B

B.1 Correction terms of turbine performance

In order to remove the dependency of the performance maps for turbine and compressor from the ambient and intake conditions, mass flow and speed terms are corrected through the following equations B.1 and B.2, respectively.

$$\dot{m}_{corr} = \dot{m} \frac{\sqrt{T_{Tin} / T_{ref}}}{P_{Tin} / P_{ref}} \tag{B.1}$$

$$N_{corr} = N * \sqrt{\frac{T_{ref}}{T_{Tin}}} \tag{B.2}$$

Correction temperature and pressure are different for turbine and compressor and constants in equations B.1 and B.2 are described in table B.1

Table B.1. Terms and definitions related to equations B.1 and B.2

N	Turbocharger speed [rpm]
$\dot{m}$	Mass flow [kg/s]
T	Temperature [K]
P	Pressure [Pa]
corr	Corrected
ref	Turbine reference (101325 Pa at 288 K)
Tin	Total inlet of turbine

References

1. Romagnoli A, Martinez-Botas R. Heat transfer analysis in a turbocharger turbine: An experimental and computational evaluation. *Applied Thermal Engineering*. 2012; 38: 58-77.

2. Tang Q, Fu J, Liu J, Boulet B, Tan L, Zhao Z. Comparison and analysis of the effects of various improved turbocharging approaches on gasoline engine transient performances. *Applied Thermal Engineering*. 2016; 93: 797-812.

3. Roethlisberger RP, Favrat D. Comparison between direct and indirect (prechamber) spark ignition in the case of a cogeneration natural gas engine, part II: engine operating parameters and turbocharger characteristics. *Applied Thermal Engineering*. 2002; 22: 1231-43.

4. Watson N, Janota S. *Turbocharging the internal combustion engine*. London: The Macmillan Press Ltd, 1982.

5. ASME. Performance Test Code on Compressors and Exhausters. *ASME Standards*. 1997.

6. Galindo J, Luján JM, Serrano JR, Hernández L. Combustion simulation of turbocharger HSDI Diesel engines during transient operation using neural networks. *Applied Thermal Engineering*. 2005; 25: 877-98.

7. Serrano JR, Arnau FJ, Dolz V, Piqueras P. Methodology for characterisation and simulation of turbocharged diesel engines combustion during transient operation. Part 1: Data acquisition and post-processing. *Applied Thermal Engineering*. 2009; 29: 142-9.

8. Rajoo S, Martinez-Botas RF. Unsteady Effect in a Nozzled Turbocharger Turbine. *Journal of Turbomachinery*. 2010; 132: 031001.

9. Bontempo R, Cardone M, Manna M, Vorraro G. Steady and unsteady experimental analysis of a turbocharger for automotive applications. *Energy Conversion and Management*. 2015; 99: 72-80.

10. Avola C, Dimitriou P, Burke R, Copeland C. Preliminary DoE Analysis and Control of Mapping Procedure for a Turbocharger on an Engine Gas-stand. *ASME Turbo EXPO 2016*. Seoul, South Korea: ASME, 2016.

11. Winterbone DE, Pearson RJ. Turbocharger turbine performance under unsteady flow - a review of experimental results and proposed models. *Sixth International Conference on Turbocharging and Air Management Systems*. London, UK: IMechE, 1998, p. 193-206.

12. Lujan JM, Galindo J, Serrano JR. Efficiency Characterization of Centripetal Turbines under Pulsating Flow Conditions. *SAE Technical Paper*. 2001.

13. Lee J, Tan CS, Sirakov B, et al. Performance Metric for Turbine Stage under Unsteady Pulsating Flow Environment. *ASME Turbo EXPO 2016*. Seoul, South Korea: ASME, 2016.

14. Ehrlich DA, Lawless PB, Fleeter S. On-Engine Turbocharger Turbine Inlet Flow Characterization. *SAE Technical Paper*. 1997.

15. Marelli S, Capobianco M. Steady and pulsating flow efficiency of a waste-gated turbocharger radial flow turbine for automotive application. *Energy*. 2011; 36: 459-65.

16. Arenz MC, Weigel B, Habermann J, et al. Development and Application of a Fast-response Total Temperature Probe for Turbomachinery. *ASME Turbo EXPO 2016*. Seoul, South Korea: ASME, 2016.

17. Lueddecke B, Filsinger D, Bargende M. Engine crank angle resolved turbocharger turbine performance measurements by contactless shaft torque detection. *11th International Conference on Turbochargers and Turbocharging*. London: IMechE, 2014, p. 301-20.

18. Laurantzon F, Tillmark N, Alfredsson PH. A pulsating flow rig for analyzing turbocharger performance. *9th International Conference on Turbochargers and Turbocharging*. 2010: 363-72.

19. Capobianco M, Marelli S. Turbocharger turbine performance under steady and unsteady flow: test bed analysis and correlation criteria. *8th International Conference on Turbochargers and Turbocharging*. London, UK: IMechE, 2006, p. 193-206.

20. Kalpakli A, Örlü R, Tillmark N, Alfredsson PH. Experimental investigation on the effect of pulsations on exhaust manifold-related flows aiming at improved efficiency. *10th International Conference on Turbochargers and Turbocharging*. 2012: 377-87.

21. Serrano JR, Arnau FJ, Dolz V, Tiseira A, Cervelló C. A model of turbocharger radial turbines appropriate to be used in zero- and one-dimensional gas dynamics codes for internal combustion engines modelling. *Energy Conversion and Management*. 2008; 49: 3729-45.

22. Piscaglia F, Onorati A, Marelli S, Capobianco M. Unsteady Behavior in Turbocharger Turbines: Experimental Analysis and Numerical Simulation. *SAE Technical Paper*. 2007.

23. Chiong MS, Rajoo S, Romagnoli A, Costall AW, Martinez-Botas RF. Integration of meanline and one-dimensional methods for prediction of pulsating performance of a turbocharger turbine. *Energy Conversion and Management*. 2014; 81: 270-81.

24. Costall A, Martinez-Botas R. Fundamental Characterization of Turbocharger Turbine Unsteady Flow Behaviour. *ASME Turbo Expo 2007*. Montreal, Canada: ASME, 2007.

25. Chiong MS, Rajoo S, Romagnoli A, Martinez-Botas R. Unsteady Performance Prediction of a Single Entry Mixed Flow Turbine Usinf 1-D Gas Dynamic Code Extended with Meanline Model. *ASME Turbo EXPO 2012*. Copenhagen, Denmark: ASME, 2012.

26. Scharf JS. Extended Turbocharger Mapping and Engine Simulation *Maschinenwesen*. Aachen: RWTH, 2010.

27. Costall AW, McDavid RM, Martinez-Botas RF, Baines NC. Pulse Performance Modeling of a Twin Entry Turbocharger Turbine Under Full and Unequal Admission. *Journal of Turbomachinery*. 2011; 133: 021005.

28. Lueckmann D, Stadermann M, Aymanns R, Pischinger S. Investigation of cross flow in double entry turbocharger turbines. *ASME Turbo EXPO 2016*. Seoul, South Korea: ASME, 2016.

29. Lee J, Tan CS, Sirakov B, et al. Performance Characterization of Twin Scroll Turbine Stage for Vehicular Turbocharger under Unsteady Pulsating Flow Environment. *ASME Turbo EXPO 2016*. Seoul, South Korea: ASME, 2016.

30. Lee EA, Varaiya P. *Structure and Interpretation of Signals and Systems*: LeeVaraiya.org, 2011.

31. Yang M, Martinez-Botas R, Rajoo S, Ibaraki S, Yokoyama T, Deng K. Unsteady behaviours of a volute in turbocharger turbine under pulsating conditions. *Global Power and Propulsion Forum 2017*. Zurich, Switzerland: GPPS, 2017.

32. Szymko S, Martinez-Botas R, Pullen KR. Experimental Evaluation of Turbocharger Turbine Performance under Pulsating Flow Conditions. *ASME Turbo EXPO 2005*. Reno-Tahoe, Nevada, USA: ASME, 2005.

33. Greitzer EM, Tan CS, Graf MB. *Internal flow: concepts and applications*. USA: Cambridge University Press, 2004.

34. Westin F. Simulation of turbocharged SI-engines - with focus on the turbine. *School of Industrial Engineering and Management*: KTH Royal Institute of Technology, 2005.

35. Ricardo. WAVE 2015.1 Help - Thermocouple Element